

Technical Report

TR-2007-007

Variational Deconvolution of Multi-Channel Images with Inequality Constraints

by

James Nagy, Martin Welk

MATHEMATICS AND COMPUTER SCIENCE

EMORY UNIVERSITY

Variational Deconvolution of Multi-Channel Images with Inequality Constraints

Martin Welk¹ and James G. Nagy²

¹ Mathematical Image Analysis Group
Faculty of Mathematics and Computer Science, Bldg. E1 1
Saarland University, 66041 Saarbrücken, Germany
welk@mia.uni-saarland.de
<http://www.mia.uni-saarland.de>

² Department of Mathematics and Computer Science
Emory University, 400 Dowman Drive, Suite W401,
Atlanta, Georgia 30322, U. S. A.
nagy@mathcs.emory.edu
<http://www.mathcs.emory.edu>

Abstract. A constrained variational deconvolution approach for multi-channel images is presented. Constraints are enforced through a reparametrisation which allows a differential geometric reinterpretation. This view point is used to show that the deconvolution problem can be formulated as a standard gradient descent problem with an underlying metric that depends on the imposed constraints. Examples are given for bound constrained colour image deblurring, and for diffusion tensor magnetic resonance imaging with positive definiteness constraint. Numerical results illustrate the effectiveness of the methods.

1 Introduction

Blurring occurs in practically every image acquisition process, due to a variety of reasons like camera and object movement, defocussing, atmospheric perturbations, optical aberrations, etc. Removing this blur and restoring undegraded images – *deblurring* – is therefore a crucial task in many application contexts, for which numerous methods have been developed. Often blurring can be described or approximated as convolution of the unknown sharp image with a fixed kernel, the *point-spread function (PSF)*. In this case, deblurring is also called *deconvolution*. A further distinction is between deconvolution with known and unknown PSF, the latter being called *blind* deconvolution.

Variational deconvolution methods aim at reconstructing the sharp image by minimising an energy functional that encodes the convolution relation between the given and sought images together with regularity assumptions on the sought image. Since typical deconvolution problems are ill-posed inverse problems, it is highly desirable to use any additional information that is available to support the sharpening process. One condition that can often be derived e.g. from physical considerations is given by inequality constraints: In a grey-value image whose

values are proportional to radiance, they are bounded from below since radiance cannot take negative values. Sometimes also an upper bound can be derived from the image acquisition parameters.

A similar situation occurs in the context of diffusion tensor magnetic resonance imaging (DTMRI), a recent three-dimensional medical imaging modality that measures, in each voxel, a symmetric 3×3 matrix that encodes the direction-dependent diffusion behaviour of water molecules in tissue. DTMRI data are highly valuable in detecting connectivity within the brain white matter which is very useful in schizophrenia or stroke studies; another potential field of application is given by heart-muscle tissue. The physical nature of the measured diffusion tensors implies that they must be positive (semi-)definite, which is an inequality constraint, too.

In this paper, we present an approach for non-blind variational deconvolution under inequality constraints. Its main component is a reparametrisation of the image range which allows a differential geometric reinterpretation. The reparametrisation principle has been used before in the context of a discrete deconvolution model [9]. We also present the extension of our framework to multi-channel images. The capabilities of the approach are demonstrated by experiments on photographic images with positivity constraints and DTMRI data with the positive definiteness constraint.

Related work. Blind or non-blind variational deconvolution has been studied by many authors, see [4, 7, 15, 1]. Though considered in a slightly different setting in 1995 [16], robust data terms have attracted broader attention recently [1], see also [14] for extensions to spatially variant PSFs and [2] for an explicit formulation with colour images. Reparametrisation has been used to impose a positivity constraint on a discrete deconvolution model in [9]. A differential geometric framework for gradient descent constrained to submanifolds (i.e. equality constraints) has been discussed in [5].

2 Variational Deconvolution with Constraints

Basic Deconvolution Model. We start from a general model for variational deconvolution of grey-value or multi-channel (colour, vector- or matrix-valued) images with spatially invariant point-spread function which is based on minimising the energy functional

$$E[u] = \int_{\Omega} \left(\Phi \left(\sum_{k \in J} (f_k - u_k * h)^2 \right) + \alpha \Psi \left(\sum_{k \in J} |\nabla u_k|^2 \right) \right) dx \quad (1)$$

where $u = (u_k)_{k \in J}$ is the image to be determined, $f = (f_k)_{k \in J}$ is the given blurred image, the index set J enumerates the image channels ($|J| = 1$ for grey-value images), and h is the uniform point-spread function for all channels. Further, Φ and Ψ are monotonically increasing functions from \mathbb{R}_0^+ to \mathbb{R} . The first summand in the integrand is the *data term* which favours images u with small reconstruction error $f - u * h$. The second summand, the *regulariser*, encourages

smoothness of the deblurred image, see also [13] for additional discussion. The *regularisation weight* $\alpha > 0$ balances the influences of both contributions.

If Φ grows slower than $\Phi(s^2) = s^2$, one speaks of a *robust data term* [1] since it reduces the influence of large residual errors (outliers) on $E[u]$ compared to a least-squares term. A typical choice is the regularised L^1 -norm $\Phi(s^2) = \sqrt{s^2 + \beta^2}$ with small $\beta > 0$. Robust data terms considerably improve the performance of variational deconvolution approaches in the presence of noise [1] or data that fulfil model assumptions imperfectly, including imprecise PSF estimates [14].

As to the regulariser, non-quadratic choices like (regularised) total variation $\Psi(s^2) = \sqrt{s^2 + \varepsilon^2}$ ($\varepsilon > 0$) [7, 4, 1] or even the non-convex Perona–Malik term $\Psi(s^2) = \lambda^2 \ln(1 + s^2/\lambda^2)$ [13] are generally favoured in the image processing literature for their edge-preserving or even edge-enhancing capabilities.

Note that in our model the channels u_k are coupled by quadratic summation in the arguments of both Ψ and Φ . While this is well-established in practice in the regulariser [11] the situation in the data term is more delicate and depends on the characteristics of noise and perturbations across the channels. A separate robustification $\sum_k \Phi((f_k - u_k * h)^2)$ as advocated in [2] can be adequate when noise is independent in the different channels, while channel-coupled noise calls for the joint robustification of (1). Due to the image acquisition procedures the latter will often apply to colour images and practically always to diffusion tensor images. Perturbations due to imperfect fulfilment of model assumptions also tend to be channel-coupled. For a discussion of joint versus separate robustification in a different context (optic flow) see also [3, p. 38].

One way to compute a minimiser of (1) is via the gradient descent

$$\partial_t u_k = \alpha \operatorname{div} \left(\Psi' \left(\sum_{l \in J} |\nabla u_l|^2 \right) \nabla u_k \right) + \left(\Phi' \left(\sum_{l \in J} (f_l - u_l * h)^2 \right) (f_k - u_k * h) \right) * \tilde{h} \quad (2)$$

where $\tilde{h}(x) := h(-x)$ denotes the PSF reflected at the origin. Starting from a suitable initial condition, which will often be the blurred image f itself, the process converges to a minimiser of (1).

We next consider how the model (1) can be modified to incorporate constraints on the solution.

Constraints for Greyvalue Images. Assume for a moment the single channel case, where the pixels represent grey-value intensities. Since negative intensities do not physically make sense, we would like to modify (1) to constrain the grey-values to be nonnegative. One obvious approach is to add a penalty for negative values, with the drawback of not strictly enforcing the inequality. Another approach, which has been shown to be very effective for discrete deconvolution problems [9], reparametrises the greyvalues via $u = \exp(z)$ with a new image function z whose values are unconstrained in \mathbb{R} , and calculates the gradient descent for z . Slightly generalising, we substitute $u = \varphi(z)$ with a smooth invertible function $\varphi : \mathbb{R} \rightarrow \mathbb{R}$ into (1) and obtain

$$\tilde{E}[z] = \int_{\Omega} \left(\Phi((f - \varphi(z) * h)^2) + \alpha \Psi\left((\varphi'(z) |\nabla z|)^2\right) \right) dx. \quad (3)$$

The gradient descent is now computed for z , after which z can be eliminated by the inverse function $z = \varphi^{-1}(u)$. This gives the new gradient descent

$$\partial_t u = \varphi'(\varphi^{-1}(u)) \left(\alpha \operatorname{div} \left(\Psi'(|\nabla u|^2) \nabla u \right) + \left(\Phi'((f-u*h)^2)(f-u*h) \right) * \tilde{h} \right) \quad (4)$$

which differs from (2) (with one channel) only by the factor $\varphi'(\varphi^{-1}(u))$ on the right-hand side.

A positivity constraint is imposed by $\varphi(z) = \exp(z)$, thus $\varphi'(\varphi^{-1}(u)) = u$. This can easily be generalised to an interval constraint $a < u < b$ by using a sigmoid function such as $\varphi(z) = \frac{a \exp(-z) + b}{\exp(-z) + 1}$, leading to $\varphi'(\varphi^{-1}(u)) = (u-a)(b-u)/(b-a)$.

Constraining Colour Images. Going from a single grey-value to multi-channel images, one notes first that constraints that act separately on the channels can be handled easily. For example, positivity or interval constraints for the channels of colour images are imposed by setting $u_k = \varphi_k(z_k)$ for $k \in J$. The corresponding gradient descent in channel k is given by equation (2) with the right-hand side multiplied by $\varphi'_k(\varphi_k^{-1}(u_k))$.

Geometric Reinterpretation. We now show that it is possible to interpret the reparametrisation approach geometrically, and this leads to a very convenient form in which more general constraints can be easily incorporated into the model. Let us consider once more grey-value images with positivity constraint, i.e. $\varphi'(\varphi^{-1}(u)) = u$. A short calculation then reveals that the right-hand side of (4) expresses the negative (variational) gradient of the *original* energy functional $E[u]$ according to (1) in a function manifold whose metric is constructed from the well-known *hyperbolic* metric $d_h u := du/u$ on the range of grey-values u , instead of the usual (Euclidean) metric. We can therefore represent our modified gradient descent process as standard gradient descent with a different underlying metric! From this viewpoint, zero and negative greyvalues are avoided simply because the hyperbolic metric puts them at infinite distance from any positive values. A similar reinterpretation is possible in the interval constraint case: Now both interval ends are pushed away to infinite distance.

Positive Definiteness Constraint in Matrix-Valued Images. As a consequence of our geometric reinterpretation, we no longer need to rely on an explicit reparametrisation of our image range to compute a constrained gradient descent. Instead, it is sufficient to calculate the gradient descent of (1) with respect to a suitably chosen metric on the image range.

This observation immediately enables us to formulate a gradient descent for variational deconvolution of matrix-valued images with positive definiteness constraint. To this end, we use the Riemannian metric on the cone of positive definite matrices that is given by $d_S A^2 = \|A^{-1/2} dA A^{-1/2}\|_F^2$ with $\|\cdot\|_F$ denoting the Frobenius norm, see [12, 6]. This metric has recently been investigated intensively in the context of DTMRI data processing, see e.g. [8, 10].

Denoting the matrix-valued image by $U = (u_k)_{k \in J}$, $J = \{1, 2, 3\} \times \{1, 2, 3\}$, the gradient descent for (1) with respect to the metric d_S is given by

$$\partial_t U = U^{1/2} G U^{1/2} \quad (5)$$

where G is the matrix of all the right-hand sides of (2) for channels $k \in J$.

3 Experiments

In our experiments, we consider a deconvolution problem for a colour image using the gradient descent (4) with $\varphi(z) = \exp(z)$, and a deconvolution problem for DTMRI data with gradient descent given by (5). We always use robust L^1 data terms. As in the case of the unconstrained gradient descent (2), a straight forward numerical implementation is through an explicit time-stepping scheme which is stopped when the updates fall below some small positive threshold. Some speedup is possible by more sophisticated schemes, but this does not affect the behaviour of the solution, which is the main focus of this paper. Also, we do not focus on experiments with additional noise since the robustness of variational deconvolution with robust data terms under e.g. impulsive noise has already been demonstrated in [1, 14].

In our first experiment (Fig. 1), we demonstrate deconvolution of a colour photograph with positivity constraint. Note that the exact PSF is unknown and slightly space-variant while a space-invariant PSF estimated from an impulse response in the image has been used for deconvolution. The ability of the method to cope with these violations of model assumptions underlines its robustness. It is evident that the positivity constraint significantly reduces oscillatory (Gibbs) artifacts along edges. Interestingly, this includes not only undershoots to negative values which are suppressed directly, but also overshoots in the positive range, due to the convolution in the data term that links over- and undershoots. We can therefore reduce the regularisation weight in the constrained deconvolution and thereby achieve reconstruction of finer details.

Our second experiment (Fig. 2) demonstrates deconvolution of matrix-valued data with positive definiteness constraint. One 2D slice of a DTMRI data set consisting of symmetric 3×3 matrices has been synthetically blurred by iterative box filtering approximating a Gaussian of standard deviation 2, and deconvolved by our method, using a Gaussian PSF of the same standard deviation.

It can be seen that many structures in the DTMRI image are nicely reconstructed by the deconvolution process, e.g. the highly anisotropic diffusion tensors of the corpus callosum region, and the sharp edges between corpus callosum and the large isotropic tensors in the adjacent ventricle. A limitation of the current method that can be seen from the figures is that very thin details with a width of only one or two voxels are still smoothed in the deconvolved image. Due to the low resolution this effect is more relevant in DTMRI data than elsewhere, and further work will be devoted to improve reconstruction quality for such details.

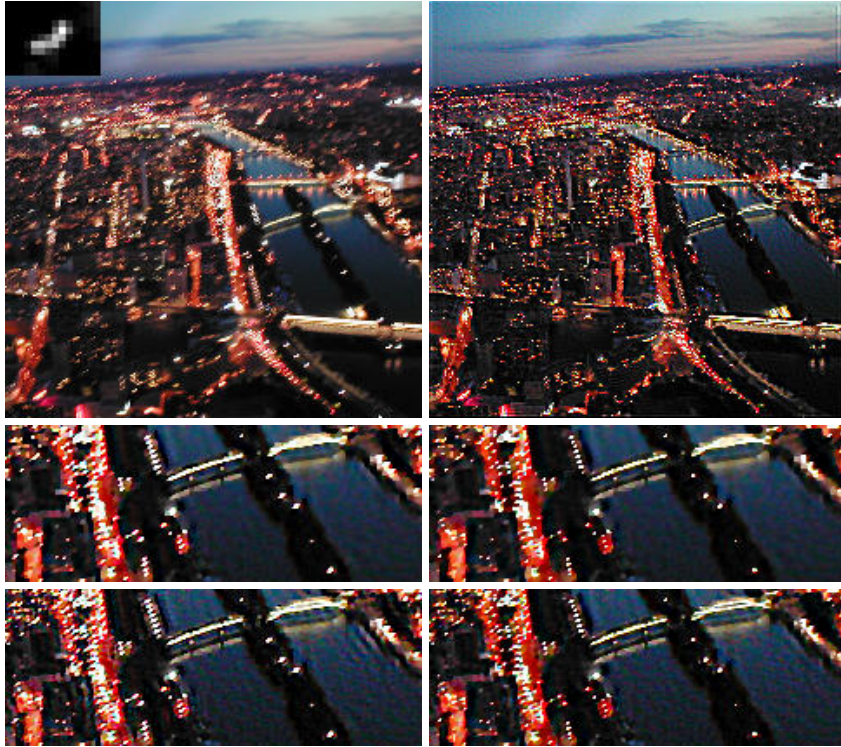


Fig. 1. **Top left:** Paris from Eiffel tower at dusk, colour photograph blurred by camera movement (480×480 pixels). *Inserted:* estimated point-spread function (enlarged). **Top right:** Variational deconvolution result with robust data term, Perona–Malik regulariser ($\lambda = 26$), regularisation weight $\alpha = 0.03$, with positivity constraint. **Middle left:** Detail (240×90 pixels) of deconvolution with the same regulariser, $\alpha = 0.06$, no constraint. **Middle right:** Same with $\alpha = 0.06$ and positivity constraint. **Bottom left:** $\alpha = 0.03$, no constraint. **Bottom right:** $\alpha = 0.03$, positivity constraint.

4 Conclusion

In this paper, we have proposed an energy minimisation approach to image deconvolution that incorporates inequality constraints, such as bounds on pixel values. Constraints are modelled either by a reparametrisation of the image values, or in a differential geometric way by modifying the metric on the image values in which a gradient descent is carried out. Particularly the second formulation allows to realise fairly general constraints on multi-channel images.

Our experiments on positivity-constrained colour image deconvolution and positive definite deconvolution of DTMRI data demonstrate the broad applicability and performance of the model.

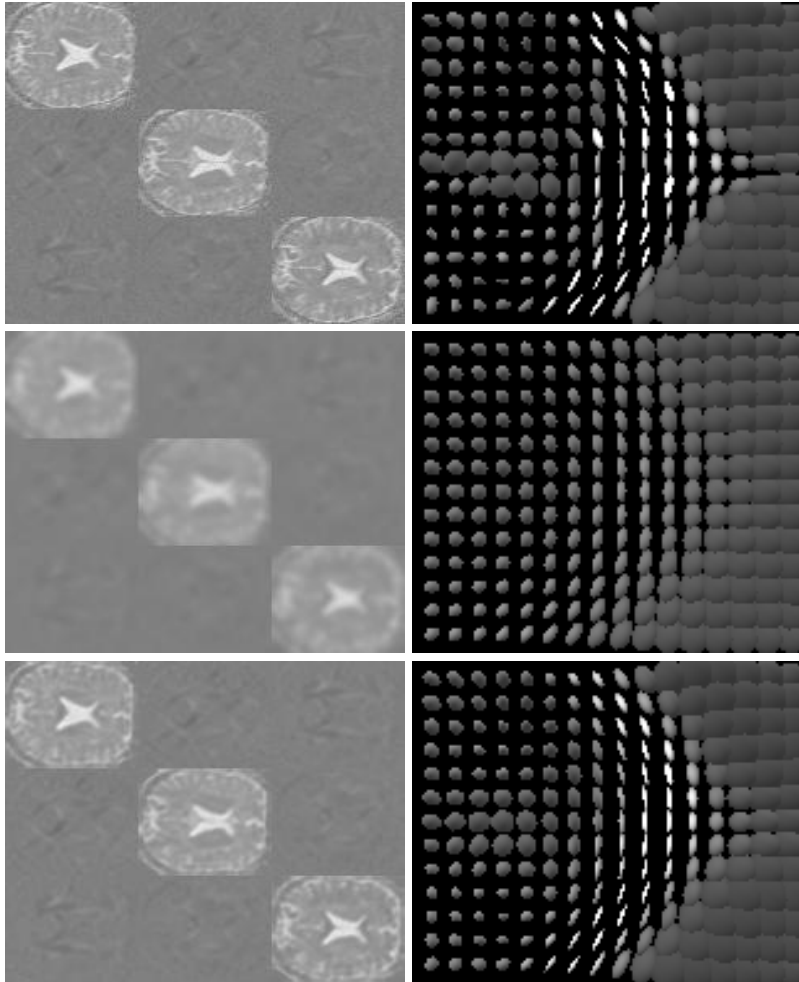


Fig. 2. **Top left:** One 2D slice from a DT-MRI data set of a human brain. The 3×3 tiles represent the matrix components, with middle grey representing 0. **Top right:** Detail from the corpus callosum region visualised by ellipsoids. Directions and lengths of the principal axes correspond to eigenvectors and eigenvalues, resp. **Middle row:** Blurred by iterated box filtering, approximating convolution with a Gaussian of standard deviation 2. **Bottom row:** Variational deconvolution with robust data terms, total variation regulariser, regularisation weight 0.03, and positive definiteness constraint.

Acknowledgements. Support of the first author by Deutsche Forschungsgemeinschaft under grant We 3563/2-1 is gratefully acknowledged. Research of the second author is supported in part by the U.S. National Science Foundation under grant DMS-05-11454. The first author also thanks Emory University for

their hospitality. The DTMRI data set has been provided by Oliver Gruber and Ilona Henseler, Saarland University Hospital, Homburg, Germany.

References

1. L. Bar, N. Sochen, and N. Kiryati. Image deblurring in the presence of salt-and-pepper noise. In R. Kimmel, N. Sochen, J. Weickert, editors, *Scale Space and PDE Methods in Computer Vision*, vol. 3459 of *Lecture Notes in Computer Science*, 107–118, Berlin, 2005, Springer
2. L. Bar, A. Brook, N. Sochen, and N. Kiryati. Color image deblurring with impulsive noise. In N. Paragios, O. Faugeras, T. Chan, C. Schnörr, editors, *Variational and Level Set Methods in Computer Vision*, vol. 3752 of *Lecture Notes in Computer Science*, 49–60, Berlin, 2005, Springer
3. A. Bruhn. *Variational Optic Flow Computation – Accurate Modelling and Efficient Numerics*. PhD thesis, Saarland University, Saarbrücken, Germany, 2006
4. T. F. Chan and C. K. Wong. Total variation blind deconvolution. *IEEE Transactions on Image Processing*, 7:370–375, 1998
5. C. Chefd’Hotel. *Méthodes Géométriques en Vision par Ordinateur et Traitement d’Image: Contributions et Applications*. PhD Thesis, ENS Cachan, France, 2004
6. S. Helgason. *Differential Geometry, Lie Groups, and Symmetric Spaces*. Academic Press, New York 1978
7. A. Marquina and S. Osher. A new time dependent model based on level set motion for nonlinear deblurring and noise removal. In M. Nielsen, P. Johansen, O. F. Olsen, and J. Weickert, editors, *Scale-Space Theories in Computer Vision*, volume 1682 of *Lecture Notes in Computer Science*, 429–434, Berlin, 1999, Springer
8. M. Moakher and P. Batchelor. Symmetric positive-definite matrices: from geometry to applications and visualization. In J. Weickert, H. Hagen, editors, *Visualization and Processing of Tensor Fields*, Berlin, 2006, Springer
9. J. G. Nagy and Z. Strakoš. Enforcing nonnegativity in image reconstruction algorithms. In D. C. Wilson et al., editors, *Mathematical Modeling, Estimation, and Imaging*, vol. 4121, 182–190, 2000
10. X. Pennec, P. Fillard, and N. Ayache. A Riemannian framework for tensor computing. *International Journal of Computer Vision*, 66(1):41–66, 2006
11. C. Schnörr. Segmentation of visual motion by minimizing convex non-quadratic functionals. In *Proc. Twelfth International Conference on Pattern Recognition*, vol. A, 661–663, Jerusalem, Israel, Oct. 1994, IEEE Computer Society Press
12. C. L. Siegel. *Symplectic Geometry*. Academic Press, New York, 1964
13. M. Welk, D. Theis, T. Brox, and J. Weickert. PDE-based deconvolution with forward-backward diffusivities and diffusion tensors. In R. Kimmel, N. Sochen, J. Weickert, editors, *Scale Space and PDE Methods in Computer Vision*, vol. 3459 of *Lecture Notes in Computer Science*, 585–597, Berlin, 2005, Springer
14. M. Welk, D. Theis, and J. Weickert. Variational deblurring of images with uncertain and spatially variant blurs. In W. Kropatsch, R. Sablatnig, A. Hanbury, editors, *Pattern Recognition*, vol. 3663 of *Lecture Notes in Computer Science*, 485–492, Berlin, 2005, Springer
15. Y.-L. You, M. Kaveh. A regularization approach to joint blur identification and image restoration. *IEEE Transactions on Image Processing*, 5(3):416–428, 1996
16. M. E. Zervakis, A. K. Katsaggelos, and T. M. Kwon. A class of robust entropic functionals for image restoration. *IEEE Transactions on Image Processing*, 4(6):752–773, 1995